Annals of Biomedical Engineering, Vol. 32, No. 7, July 2004 (©2004) pp. 911–923

Adult Stem Cell Driven Genesis of Human-Shaped Articular Condyle

ADEL ALHADLAQ,[1] JENNIFER H. ELISSEEFF,[2] LIU HONG,[1] CHRISTOPHER G. WILLIAMS,[2]
ARNOLD I. CAPLAN,[3] BLANKA SHARMA,[2] ROSS A. KOPHER,[1] SARA TOMKORIA,[1]
DONALD P. LENNON,[3] AURORA LOPEZ,[1] and JEREMY J. MAO[1]

[1]Tissue Engineering Laboratory, Departments of Anatomy and Cell Biology, Bioengineering, and Orthodontics, University of Illinois at Chicago, Chicago, IL; [2]Departments of Biomedical Engineering and Plastic Surgery, Johns Hopkins University, Baltimore, MD; and [3]Skeletal Research Center, Department of Biology, Case Western Reserve University, Cleveland, OH

(Received 10 October 2003; accepted 20 February 2004)

Abstract—Uniform design of synovial articulations across mammalian species is challenged by their common susceptibility to joint degeneration. The present study was designed to investigate the possibility of creating human-shaped articular condyles by rat bone marrow-derived mesenchymal stem cells (MSCs) encapsulated in a biocompatible poly(ethylene glycol)-based hydrogel. Rat MSCs were harvested, expanded in culture, and treated with either chondrogenic or osteogenic supplements. Rat MSC-derived chondrogenic and osteogenic cells were loaded in hydrogel suspensions in two stratified and yet integrated hydrogel layers that were sequentially photopolymerized in a human condylar mold. Harvested articular condyles from 4-week *in vivo* implantation demonstrated stratified layers of chondrogenesis and osteogenesis. Parallel *in vitro* experiments using goat and rat MSCs corroborated *in vivo* data by demonstrating the expression of chondrogenic and osteogenic markers by biochemical and mRNA analyses. *Ex vivo* incubated goat MSC-derived chondral constructs contained cartilage-related glycosaminoglycans and collagen. By contrast, goat MSC-derived osteogenic constructs expressed alkaline phosphatase and osteonectin genes, and showed escalating calcium content over time. Rat MSC-derived osteogenic constructs were stiffer than rat MSC-derived chondrogenic constructs upon nanoindentation with atomic force microscopy. These findings may serve as a primitive proof of concept for ultimate tissue-engineered replacement of degenerated articular condyles via a single population of adult mesenchymal stem cells.

Keywords—Mesenchymal, Cartilage, Bone, Tissue engineering, Stem cell, Osteochondral, Hydrogel.

INTRODUCTION

The design of the articular condyle of the synovial joint is intriguing in that cartilage and bone, two distinct adult tissue phenotypes with little in common, structurally integrate and function in synchrony to withstand mechanical loading up to several times body weight.[45] However, the uniform design of synovial condyles across species has been met with rigorous challenges of not only diverse functional demands, but also a common susceptibility to pathologic conditions. The chondral and osseous structures of synovial joints can deteriorate, resulting from injuries, rheumatoid arthritis, or osteoarthritis, all of which are debilitating disorders in humans and other species.[22,26,50] Injuries and arthritis necessitate more than 400,000 total joint replacement procedures each year in the United States alone.[40] Despite certain levels of clinical success, total joint replacement by auto-, allo-, and xeno-grafts as well as synthetic materials suffer from deficiencies such as donor site morbidity, immunorejection, limited tissue supply, transmission of pathogens, and metal loosening, wear and tear.[2,30,55] Tissue engineering of bone and cartilage has the potential to overcome these deficiencies and has been regarded as the next frontier in regenerative medicine.[40,46] Indeed, cartilage regeneration by means of isolated chondrocytes or resurfacing of surgically created cylindrical articular defects has shown encouraging results in animal models.[9,18,23,62] Bone regeneration by encapsulating mesenchymal stem cells and/or growth factors in polymer scaffolds has shown considerable promise toward tissue-engineered repair of bony defects.[10,31,43,58,65] However, it remains an unmet challenge to engineer a composite stem cell-driven osteochondral construct molded into the form of a human articular condyle that may ultimately be used in total joint replacement.

Cartilage- and bone-forming cells, chondrocytes and osteoblasts, respectively, derive from the common progenitor of mesenchymal stem cells.[7,12,23,38,53] The biologic characteristics of cartilage and bone dictate that a tissue-engineered osteochondral construct aimed at replacing the entire articular condyle must be formed *de novo* by progenitor cells that have already committed to chondrogenic and osteogenic lineages. Stem cells are necessary because full-thickness osteochondral defects, such as those

Address correspondence to Jeremy Mao, DDS, PhD, Director and Associate Professor, Tissue Engineering Laboratory MC 481, Departments of Anatomy and Cell Biology, Bioengineering, and Orthodontics, University of Illinois at Chicago, Chicago, IL 60612. Electronic mail: jmao2@uic.edu

in osteoarthritis, heal poorly in the absence of corresponding tissue-forming cells.[14,34,42] Adult mesenchymal stem cells have advantages over embryonic stem cells for tissue engineering of osteochondral constructs because adult MSCs readily differentiate into both chondrogenic and osteogenic cells. Previous attempts to fabricate osteochondral constructs have utilized several meritorious approaches that inspired various components of the present work. Much has been learned from the repair of surgically created cylindrical osteochondral defects of the articular condyle by chondral or osteochondral constructs loaded with articular chondrocytes and periosteal cells or marrow-derived cells in biocompatible polymers.[21,56,57,60] Human-shaped phalanges consisting of multiple joints have been formed in athymic mice by seeding chondrocytes and tenocytes in a biodegradable polymer scaffold and wrapped with the periosteum.[35] A synovial condyle was formed from marrow-derived osteogenic cells but lacked the cartilage component.[1] Here, we report *de novo* formation of an articular condyle in the shape and dimensions of a human condyle with both cartilaginous and osseous components from a single population of adult mesenchymal stem cells encapsulated in a photopolymerizable poly(ethylene glycol)-based hydrogel.

MATERIALS AND METHODS

Isolation and Culture of Rat and Goat Marrow-Derived Mesenchymal Stem Cells

Rat bone marrow-derived MSCs were isolated from 2–4-month-old (200–250 g) male Sprague-Dawley rats (Harlan, Indianapolis, IN). Following CO_2 asphyxiation, the tibia and femur were dissected (Fig. 1(A)). Whole bone marrow plugs were flushed out with a 10-ml syringe filled with Dulbecco's Modified Eagle's Medium-Low Glucose medium (DMEM-LG; Sigma, St. Louis, MO) supplemented with 10% fetal bovine serum (FBS) (Biocell, Rancho Dominguez, CA) and 1% antibiotic-antimycotic (Gibco, Carlsbad, CA). Marrow samples were collected and mechanically disrupted by passage through 16-, 18-,

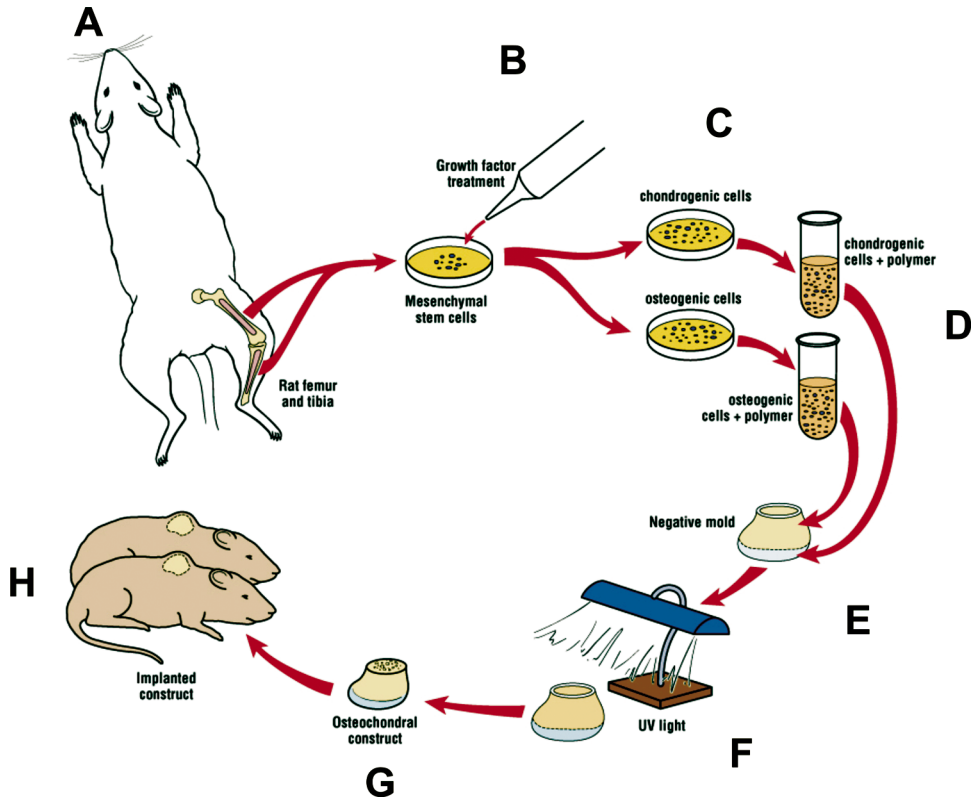

FIGURE 1. Experimental protocol for tissue-engineered articular condyles with both cartilaginous and osseous components from a single population of mesenchymal stem cells. (A) Harvest of mesenchymal stem cells (MSCs) from the rat tibiofemoral complex. (B) Expansion of primary MSCs in culture. (C) Treatments of a single population of expanded MSCs with chondrogenic medium containing TGF-β1, and osteogenic medium containing dexamethasone, β-glycerophosphate, and ascorbic acid. (D) Separate PEG-hydrogel suspensions of MSC-derived chondrogenic and osteogenic cells. (E) Loading of PEG-hydrogel suspension with MSC-derived chondrogenic cells in lower portion of the negative mold of the articular condyle (approx. thickness: 2 mm; cf. Fig. 2(C)) followed by photopolymerization with UV light (F). Then, PEG-hydrogel suspension with MSC-derived osteogenic cells was loaded to occupy the upper portion of the negative mold of the articular condyle followed by photopolymerization. The fabricated osteochondral constructs (G) were implanted in subcutaneous pockets in the dorsum of immunodeficient mice (H).

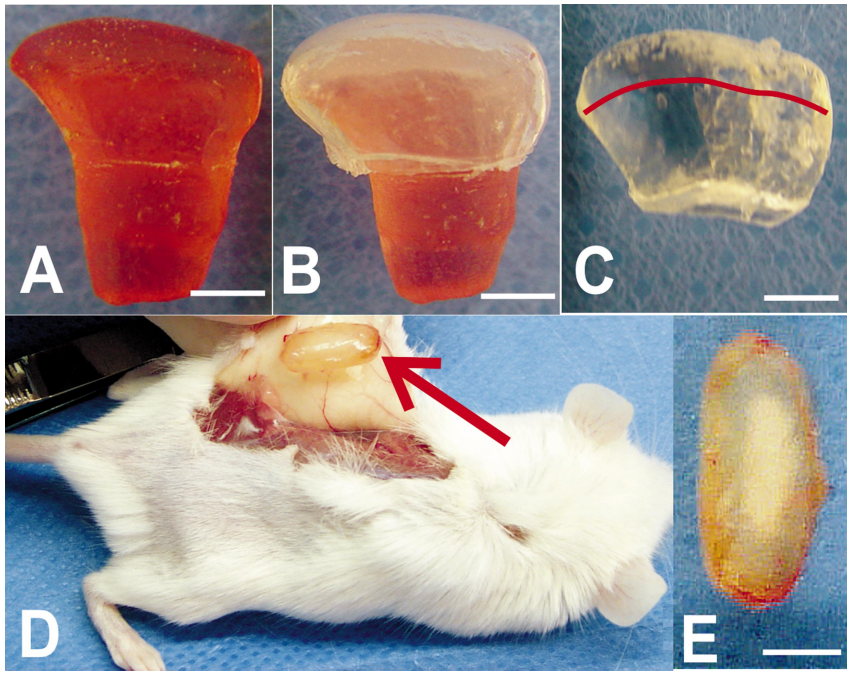

FIGURE 2. Fabrication and tissue engineering of a human-shaped articular condyle from rat bone marrow-derived mesenchymal stem cells. (A) Acrylic model made from alginate impression of a human cadaver mandibular condyle. (B) Polyurethane negative mold fits the acrylic human articular condyle model. (C) A poly(ethylene glycol)-based hydrogel construct of the human mandibular condyle was fabricated in a two-phase process: (1) PEG-hydrogel solution encapsulating MSC-derived chondrogenic cells was loaded to occupy the top 2 mm of the negative mold (above the thin red line) followed by photopolymerization; and (2) additional PEG-hydrogel solution encapsulating MSC-derived osteogenic cells was loaded to occupy the remaining 5 mm space below the red line followed by photopolymerization. (D) Harvest of tissue-engineered articular condyle after 4-week subcutaneous implantation of the osteochondral construct in the dorsum of immunodeficient mice. (E) Harvested osteochondral construct retained the shape and dimensions of the molded articular condyle. Transparent and photo-opaque portions of the construct represent cartilaginous and osseous components of the tissue-engineered articular condyle as evidenced by histologic characteristics of the chondral and osseous components in Fig. 2. Scale bar: 3 mm.

and 20-gauge needles. Cells were centrifuged, resuspended in serum-supplemented medium, counted and plated at 5×10^7 cells/100-mm culture dish and incubated in 95% air/5% CO_2 at 37°C, with fresh medium change every 3–4 days (Fig. 1(B)). When large colonies were formed (typically 2–3 weeks), primary MSCs were trypsinized, counted, and passaged at a density of $5–7 \times 10^5$ cells/100-mm dish. Rat MSCs were used to tissue-engineer the human-shaped articular condyles *in vivo* (Figs. 2 and 3) and to fabricate the *ex vivo* chondrogenic and osteogenic constructs that were separately prepared for nanomechanical analysis (Fig. 7). All animal experiments received appropriate approval from the institutional Animal Care Committee.

Goat MSCs were isolated from femoral bone marrow aspirated into 10-ml syringes of approximately 3-year-old, castrated male goats. Marrow samples were washed and centrifuged twice (1000 rpm for 10 min) in mesenchymal stem cell growth medium (BioWhittaker, Walkersville, MD). Cells were counted and plated in 75-cm^2 flasks at a density of 12,000 cells/cm^2. Cultures were incubated in 95% air/5% CO_2 at 37°C with the first medium change occurred at day 4 and then every 2–3 days until near confluency. Cells were passaged with 0.025% Trypsin/EDTA (BioWhittaker, Walkersville, MD) for 5 min at 37°C and replated in 75 cm^2 at 5000 cells/cm^2. Goat MSCs were utilized to prepare the *ex vivo* incubated constructs that were used to demonstrate the chondrogenic and osteogenic processes *in vitro*, including biochemical and genetic analysis in this study (Figs. 5 and 6).

Chondrogenic and Osteogenic Differentiation of Marrow-Derived Mesenchymal Stem Cells

Chondrogenic or osteogenic supplements were applied separately to first passage MSCs in DMEMLG + 10% FBS for 1 week. Chondrogenic supplement consisted of 10 ng/ml TGF-β1 (RDI, Flanders, NJ), whereas osteogenic supplement consisted of 100 nM dexamethasone, 10 mM β-glycerophosphate, and 0.05 mM ascorbic acid-2-phosphate (Sigma) (Fig. 1(B) and 1(C)). First passage rat and goat MSCs were exposed to the same formulated chondrogenic and osteogenic supplements. Cultures were incubated in 95% air/5% CO_2 at 37°C with medium changes every 3–4 days.

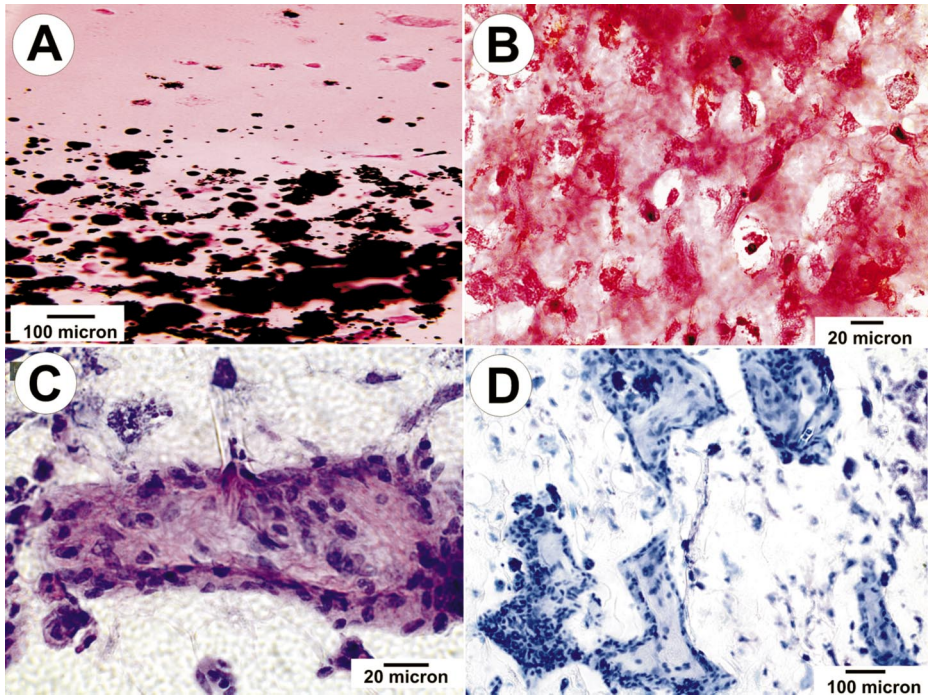

FIGURE 3. Representative photomicrographs of a tissue-engineered articular condyle from rat bone marrow derived MSCs harvested after 4 weeks of *in vivo* implantation in immunodeficient mice. (A) Von Kossa stained section of the osteochondral interface of tissue-engineered articular condyle. The upper 1/3 of "A" represents the chondrogenic portion characterized by abundant intercellular space between MSC-derived chondrocyte-like cells. The lower 2/3 of "A" represents the osteogenic portion characterized by abundant mineralization nodules. (B) Positive safranin O red stain indicates the presence of cartilage-related glycosaminoglycans in the intercellular matrix of the chondral portion of the tissue-engineered articular condyle. (C) H&E stained section from the osseous portion of the construct showing a representative island of bone trabecula-like structure populated by MSC-derived osteoblast-like cells. (D) Toluidine blue staining of trabecula-like structures in the osseous portion of the tissue-engineered articular condyle.

Hydrogel Preparation, Cell Encapsulation, and Fabrication of Condyle-Shaped Osteochondral Constructs

Poly(ethylene glycol) diacrylate (PEGDA) (MW 3400; Shearwater Polymers, Huntsville, AL) was dissolved in sterile PBS supplemented with 100 units/ml penicillin and 100 μg/ml streptomycin (Gibco, Carlsbad, CA) to a final solution of 10% w/v. A photoinitiator, 2-hydroxy-1-[4-(hydroxyethoxy)phenyl]-2-methyl-1-propanone (Ciba, Tarrytown, NY), was added to the PEGDA solution to obtain a final initiator concentration of 0.05% w/v. Rat MSC-derived chondrogenic and osteogenic cells were trypsinized, counted, and resuspended in PEGDA polymer/photoinitiator solution at a concentration of 5×10^6 cells/ml (Fig. 1(D)). A 200-μl aliquot of cell/polymer suspension with MSC-derived chondrogenic cells was loaded into a hollow polyurethane mold of a cadaver human mandibular condyle with an overall dimension of $11 \times 6 \times 7$ mm ($l \times w \times h$) (Fig. 1(E)). The chondrogenic layer was photopolymerized by a long-wave, 365-nm ultraviolet lamp (Glowmark, Upper Saddle River, NJ) at an intensity of $\sim$4 mW/cm^2 (Fig. 1(F)). Cell/polymer suspension containing MSC-derived osteogenic cells (approx. 400 μl) was subsequently loaded to occupy the remainder of the condylar mold followed by the same protocol of photopolymerization (Fig. 1(E) and 1(F)).

In Vivo Implantation of Osteochondral Constructs

Severe combined immunodeficient (SCID) mice (Harlan, Indianapolis, IN) were anesthetized with IP injection of 100 mg/kg ketamine plus 5 mg/kg xylazine. The polymerized osteochondral constructs (Fig. 1(G)) were removed from the mold, washed twice with PBS, and implanted in subcutaneous pockets in the dorsum of SCID mice prepared by blunt dissection.

Ex Vivo Incubation of MSC-Derived Chondrogenic and Osteogenic Cells in PEG-Based Hydrogel Constructs

Goat MSCs were used to prepare single-layered chondrogenic or osteogenic constructs separately for *in vitro* analysis of chondrogenesis or osteogenesis, respectively. Rat MSCs were used to prepare chondrogenic and osteogenic constructs separately for nanomechanical analysis. MSC-derived chondrogenic and osteogenic cells were trypsinized, counted, and separately resuspended in PEGDA polymer/photoinitiator solution at a concentration of 20×10^6 cells/ml. Chondrogenic and osteogenic

cell/polymer suspension aliquots (approx. 150 μl each) were loaded separately in tissue culture inserts (6-mm diameter) and UV-photopolymerized as described above. Resultant hydrogel constructs were placed in 12-well tissue culture plates and incubated with either chondrogenic or osteogenic supplement as described above.

Cell Viability Assays

Cell viability after encapsulation and polymerization processes was demonstrated by using live/dead viability/cytotoxicity kit (Molecular Probes, L-3224, Eugene, OR). Briefly, calcein diffused through cell membrane and reacted with intracellular esterase to produce green fluorescence, whereas ethidium homodimer diffused only through damaged cell membrane and bound to nucleic acids to produce red fluorescence.

Histologic Tissue Phenotyping

Harvested osteochondral constructs following 4-week *in vivo* incubation were prepared by using standard histological procedures. Sequential microscopic sections were stained with hematoxylin and eosin, toluidine blue, von Kossa, and safranin-O/fast green (Sigma) to distinguish osseous and cartilaginous tissue phenotypes.

Biochemical Analysis

Goat MSCs were encapsulated in all the constructs used for biochemical analysis. Following 0, 3, and 6 weeks of *ex vivo* incubation, wet weights (ww) and of *ex vivo*-incubated chondrogenic and osteogenic constructs ($N =$ 3–4 each) were obtained and dry weights (dw) were obtained after 48 h of lyophilization. The dried constructs were crushed and digested in 1 ml of papainase (Papain, [125 μg/ml; Worthington Biomedical, Lakewood, NJ], 100 mM PBS, 10 mM cysteine, and 10 mM EDTA, pH 6.3) for 18 h at 60°C. Cell count was determined by measuring the DNA content (ng of DNA/mg dw of the hydrogel) using Hoechst 33258. Glycosaminoglycan (GAG) content was estimated by chondrotin sulfate using dimethylmethylene blue dye. Total collagen content was determined by measuring the hydroxyproline content after acid hydrolysis and reaction with *p*-dimethylaminobenzaldehyde and chlorimine-T using 0.1 as the ratio of hydroxyproline to collagen. Calcium content was measured using Sigma Kit 587 ($N =$ 3–4). Statistical significance was determined by ANOVA and post hoc Bonferroni test at an alpha level of 0.05.

RNA Extraction and Reverse Transcription-Polymerase Chain Reaction (RT-PCR)

Goat MSCs were encapsulated in all the constructs used for RT-PCR analysis. Total RNA was isolated from *ex vivo*-incubated hyrdogel constructs using RNeasy Kit (Qiagen, Valencia, CA). The constructs were homogenized (pellet pestle mixer; Kimble/Kontes, Vineland, NJ) in 1.5-ml microcentrifuge tubes containing 200 μl of RLT buffer. Then 400 μl RLT buffer was added followed by further homogenization with the QIAshredder (Qiagen) column. The homogenates were transferred to columns after addition of an equal volume of 70% ethanol. The RNA was reverse-transcribed into cDNA using random hexamers with the superscript amplification system (Gibco). One-microliter aliquots of the resulting cDNA were amplified in 50 μl volume at annealing temperature of 58°C (collagen type II was annealed at 60°C) for 35 cycles using the Ex Taq DNA Polymerase Premix (Takara Bio, Otsu, Shiga, Japan). PCR primers (forwards and backwards, 5′ to 3′) were as follows: and β-actin, 5′-TGGCACCACACCTTCTACAATGAGC-3′ and 5′-GCACAGCTTCTCCTTA ATGTCACGC-3″; osteonectin, 5′-ACGTGGCTAAGAATGTCATC-3′ and 5′-CTGGT-AGGCGA-3′; and alkaline phosphatase, 5′-ATG-AGGGCCTGGATCTTCTT-3′ and 5′-GCTTCTGCTTCT-GAGTCAGA-3′. Each PCR product was analyzed by separating 4 μl of the amplicon and 1 μl of loading buffer in a 2% agarose gel in TAE buffer. Relative band intensities of the genes of interest were compared to those of the housekeeping gene.

Measuring Nanomechanical Properties with Atomic Force Microscopy (AFM)

Rat MSCs were encapsulated in all the constructs used for nanomechanical analysis. Following 4 weeks of *ex vivo* incubation, hydrogel constructs incubated in chondrogenic or osteogenic medium were subjected to nanoindentation with Nanoscope IIIa atomic force microscope (AFM) (Veeco-Digital Instruments, Santa Barbara, CA). Hydrogel constructs, with no cells encapsulated and incubated in DMEM, served as controls. All constructs were prepared in approximately $3 \times 3 \times$ 3 mm blocks. Force spectroscopy images were obtained in contact mode using AFM fluid chamber by driving the cantilever tip in the Z plane and were used to calculate the force of indentation represented by the amount of the tip deflection from the sample's surface. Cantilevers with a nominal force constant of $k =$ 0.12 N/m and oxide-sharpened Si_3N_4 tips were used to apply nanoindentation against the construct's surface.[33,49] Randomly selected areas ($N =$ 8–12) on each sample's surface were scanned using scan rate and scan size of 14 Hz and 50 μm^2, respectively. Force mapping involved data acquisition of nanoindentation load and corresponding displacement in the Z plane during both extension and retraction of the cantilever tip.[33,49] Young's modulus (E) was calculated from force spectroscopy data using the Hertz model,[33,49] which defines a relationship between contact radius, the nanoindentation load, and the central displacement:

$$E = \frac{3F(1-\nu^2)}{4\sqrt{R}\delta^{3/2}},$$

where E is the Young's modulus, F is the applied nanomechanical load, ν is the Poisson's ratio for a given region, R is the radius of curvature of the AFM tip, and δ is the amount of indentation. The Poisson's ratios for hydrogel, chondrogenic, and osteogenic constructs were all derived from previous studies.[6,15,19,28,33,37,66] Differences in average Young's moduli among PEG hydrogel alone, PEG hydrogels encapsulating MSC-derived chondrogenic and osteogenic cells were detected by ANOVA and post hoc Bonferroni test at an alpha level of 0.01.

RESULTS

Tissue-Engineered Articular Condyles In Vivo

De novo formation of the articular condyle-like structures in a dimension of $11 \times 6 \times 7$ mm ($l \times w \times h$) was observed after a 4-week *in vivo* implantation of osteochondral constructs consisting of rat MSC-derived chondrogenic and osteogenic cells encapsulated in two stratified layers of poly(ethylene glycol)-based hydrogel (PEG hydrogel) in the subcutaneous pockets of the dorsum of immunodeficient mice (Fig. 2(D)). The harvested articular condyles from *in vivo* implantation (Fig. 2(E)) resembled the macroscopic shape and dimensions of the cell-hydrogel construct (Fig. 2(C)) as well as the positive and negative condylar molds (Fig. 2(A) and 2(B)). There were a superficial transparent portion and an inner photo-opaque portion in the superior view of the harvested articular condyle (Fig. 2(E)), representing chondrogenic and osteogenic elements, respectively, as evidenced below.

Histologic Tissue Phenotypes

The interface between the upper layer PEG hydrogel encapsulating MSC-derived chondrogenic cells and the lower layer encapsulating MSC-derived osteogenic cells (cf., above and below the red line in Fig. 2(C)) demonstrated distinctive microscopic characteristics (Fig. 3). The chondrogenic and osteogenic portions of the PEG hydrogel remained in their respective layers without substantial migration into each other's territories (cf., interface in Fig. 3(A)). The chondrogenic layer contained sparse chondrocyte-like cells surrounded by abundant intercellular matrix (Fig. 3(B)). The intercellular matrix of the chondrogenic layer showed positive reaction to safranin O (Fig. 3(B)), a cationic chondrogenic marker that binds to cartilage-related GAGs such as chondroitin sulfate and keratan sulfate.[39,64] Some of the MSC-derived chondrogenic cells were surrounded by pericellular matrix, characteristic of natural chondrocytes (Fig. 3(B)). By contrast, the osteogenic layer contained mineralization nodules that were confirmed to be mineral crystals by von Kossa staining (lower portion of Fig. 3(A)). The osteogenic layer also showed multiple island structures occupied by osteoblast-like cells as exemplified in Fig. 3(C). These island structures stained blue with toluidine blue staining (Fig. 3(D)). The chondrogenic layer showed negative staining to osteogenic markers such as von Kossa, whereas the osteogenic layer demonstrated negative reactions to chondrogenic markers such as safranin O (data not shown).

Vitality of MSCs following Photoencapsulation in PEG-Based Hydrogel

Marrow-derived MSCs adhered to the culture plate and demonstrated typical spindle shape following first passage monolayer culture (Fig. 4(A)). The majority of encapsulated MSCs in the PEG-based hydrogel remained viable after photopolymerization as demonstrated by fluorescent live-dead cell staining (live cells labeled green with calcein) (Fig. 4(B)).

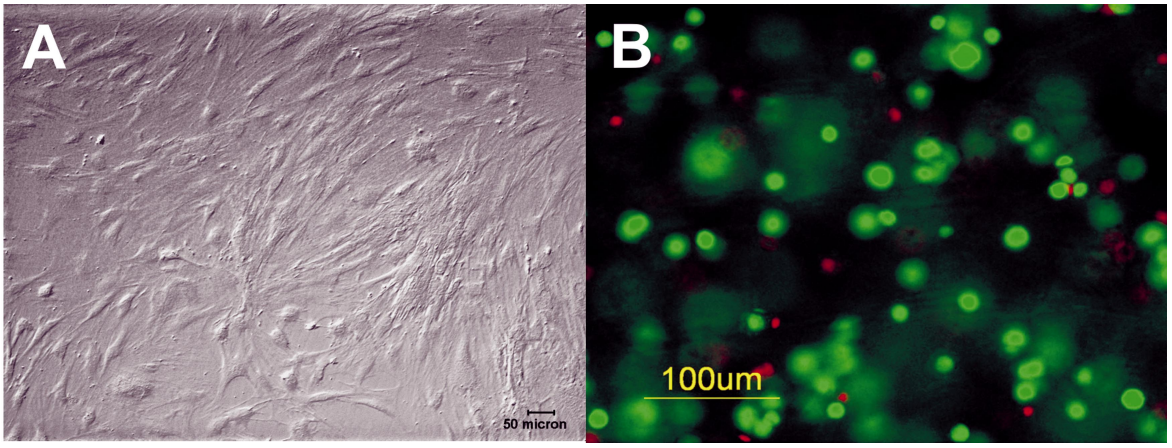

FIGURE 4. Monolayer culture and photoencapsulation of mesenchymal stem cells (MSCs). (A) Primary rat MSCs culture-expanded for 2 weeks adhered to culture plate. (B) The majority of encapsulated MSCs in the PEG-based hydrogel remained viable after photopolymerization as demonstrated by fluorescent live-dead cell staining (live cells labeled green with calcein).

MSC-Driven Chondrogenesis in PEG-Based Hydrogel Ex Vivo

Goat MSC-derived chondrogenic cells photoencapsulated in PEG-based hydrogel showed positive safranin O reaction, especially in their pericellular matrix (Fig. 5(A)), indicating synthesis of cartilage-related glycosaminoglycans.[39,64] Both GAG and total collagen contents demonstrated significant increases following 3 and 6 weeks of incubation of goat MSC-derived chondrogenic cells encapsulated in PEG-based hydrogel in the chondrogenic medium, in comparison with Day 0 ($P < 0.05$) (Fig. 5(B) and 5(C), respectively). DNA fraction analysis of the PEG-based hydrogel constructs encapsulating goat MSC-derived chondrogenic cells incubated in the chondrogenic medium revealed approximately consistent cell survival rates over the 6-week incubation period (Fig. 5(D)). The chondrogenic constructs did not express osteogenic markers such as alkaline phosphatase and osteonectin (data not shown).

MSC-Driven Osteogenesis in PEG-Based Hydrogel Ex Vivo

Monolayer goat MSCs cultured 4 weeks in the osteogenic medium showed positive reaction to alkaline phosphatase as exemplified in Fig. 6(A). Goat MSC-derived osteogenic cells encapsulated in PEG hydrogel incubated 4 weeks in the osteogenic medium reacted positively to von Kossa staining and contained mineral nodules (Fig. 6(B)), and expressed osteonectin and alkaline phosphatase genes by RT-PCR analysis (Fig. 6(C)). A quantitative calcium assay revealed significant increases in calcium content in MSC-derived osteogenic constructs as a function of incubation time in osteogenic medium from 0 to 6 weeks ($P < 0.05$) (Fig. 6(D)). The osteogenic construct did not express chondrogenic markers such as aggrecan and type II collagen genes (data not shown). DNA fraction analysis revealed relatively consistent cell survival rates over the 6-week incubation period of the hydrogel constructs encapsulating goat MSC-derived osteogenic cells (Fig. 6(E)).

Nanomechanical Properties of Chondrogenic and Osteogenic Constructs

Rat MSC-derived chondrogenic and osteogenic cells were encapsulated separately in PEG hydrogel constructs and incubated in chondrogenic or osteogenic medium, respectively, for 4 weeks and then subjected to nanoindentation with atomic force microscope (AFM). Three typical force–displacement curves for PEG hydrogel (Fig. 7(A)), PEG hydrogel with MSC-derived chondrogenic cells (Fig. 7(B)), and PEG hydrogel with MSC-derived osteogenic cells (Fig. 7(C)) demonstrated different nanoindentation forces upon both approaching and retracting phases of the AFM scanning tip. Chondrogenic and osteogenic constructs showed significantly different Young's moduli ($P < 0.01$) (Fig. 7(D)), which are defined as the slope of the stress versus strain curve and represent the elastic mechanical properties of the material under study. The average Young's modulus of osteogenic constructs was 582 ± 59 kPa (kPa $\pm$ SD), significantly higher than chondral constructs (329 ± 54 kPa) ($P < 0.01$), which in turn was significantly higher than PEG hydrogel alone (166 ± 23 kPa) ($P < 0.01$) (Fig. 7(D)). These nanomechanical data suggest that MSC-derived osteogenic cells encapsulated in PEG hydrogel have produced stiffer matrices than matrices synthesized by MSC-derived chondrogenic cells, both of which are significantly stiffer than PEG hydrogel alone.

DISCUSSION

The present data demonstrate *de novo* formation of articular condyles in the shape and dimensions of a natural human articular condyle with both cartilaginous and osseous components from a single population of adult rat bone marrow-derived MSCs encapsulated in two stratified layers of a uniform PEG-based hydrogel. The outcome of the present study is consistent with our recent work demonstrating *de novo* formation of human-shaped articular condyles from a single population of mesenchymal stem cells.[4] The present work provides more detailed characterization of tissue-engineered chondrogenic and osteogenic structures, a task that we pointed out as the next step in our previous work.[4] The dimensions of the tissue-engineered articular condyle likely are a critical factor because cell survival is anticipated to be increasingly challenging in polymer materials with increasing dimensions.[41] Stratified chondrogenesis and osteogenesis as evidenced by histological phenotypes in the present study indicate that the majority of MSC-differentiated chondrogenic and osteogenic cells not only have survived an array of *ex vivo* and *in vivo* procedures, but also have synthesized corresponding chondral and osseous matrices. The present approach of tissue-engineered articular condyles from a single population of adult mesenchymal stem cells in the shape and dimensions of human articular condyle may help our understanding toward eventual therapeutic applications in patients suffering from osteo- and rheumatoid arthritis. Currently, the regenerative outcome of natural allogenic osteochondral constructs from patients is superior to cartilage resurfacing techniques in treating large osteochondral lesions.[2,5] Tissue-engineered osteochondral constructs are expected to overcome the deficiencies associated with natural allogenic osteochondral grafts.[40,46] Previous attempts to tissue-engineer osteochondral composites have utilized tissue-forming cells from multiple sources.[5,21,35,56,57] Cotransplantation of isolated bovine articular chondrocytes and rat calvarial osteoblasts in alginate constructs resulted in the formation of both cartilaginous

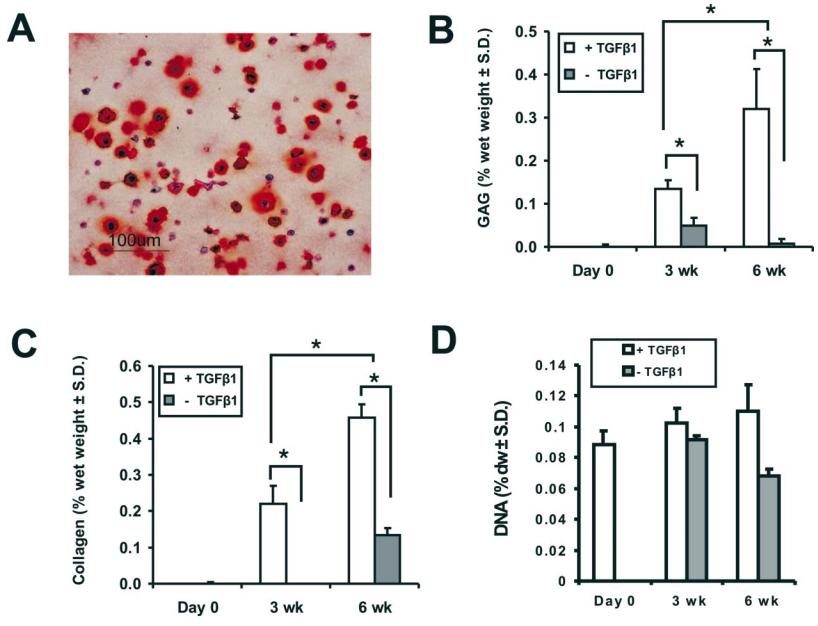

FIGURE 5. TGFβ1-mediated, MSC-driven chondrogenesis in PEG-based hydrogel constructs. (A) Goat MSC-derived chondrogenic cells encapsulated in PEG hydrogel and incubated in chondrogenic medium for 4 weeks showed positive safranin O staining. (B and C) Chondrogenesis is further indicated by increases in total GAG content (B) and total collagen content (C) in PEG hydrogel encapsulating MSC-derived chondrogenic cells following 0, 3, and 6 weeks of incubation in chondrogenic medium containing TGF-β1 ($P < 0.05$). (D) DNA content analysis of the PEG-based hydrogel constructs encapsulating goat MSC-derived chondrogenic cells incubated in the chondrogenic medium in the presence of TGF-β1 revealed approximately consistent cell survival rates over the 6-week incubation period.

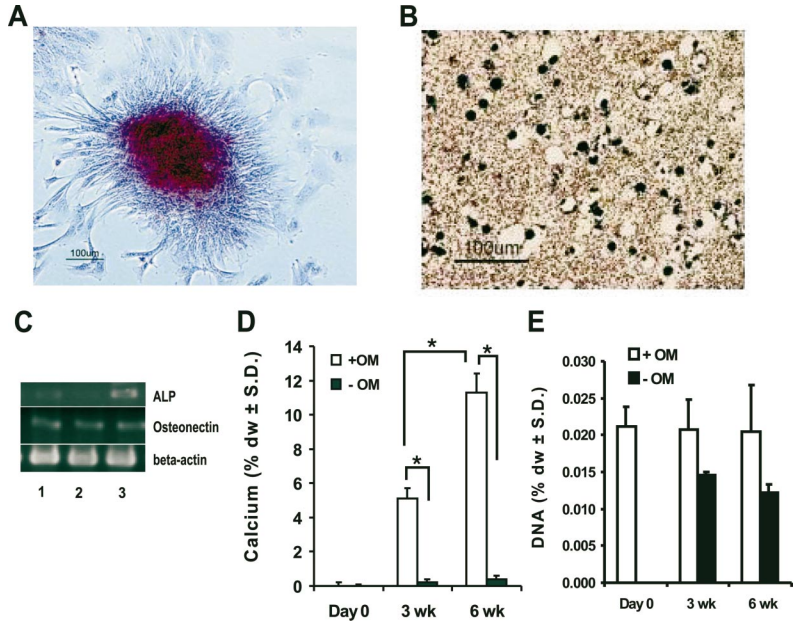

FIGURE 6. MSC-driven osteogenesis in monolayer culture and after encapsulation in PEG hydrogel upon induction by osteogenic medium containing dexamethasone, β-glycerophosphate, and ascorbic acid. (A) Positive reaction of goat MSCs in monolayer culture to alkaline phosphatase after 4-week treatment with osteogenic medium. (B) Matrix mineral deposition in PEG hydrogel encapsulating goat MSCs evidenced by positive reaction to von Kossa silver staining after 4-week incubation in osteogenic medium. (C) expression of alkaline phosphatase and osteonectin genes as a function of incubation periods of PEG hydrogel encapsulating goat MSCs in osteogenic medium (Lane 1: 1-week incubation; Lane 2: 3-week incubation; Lane 3: 6-week incubation). (D) Increasing calcium content in PEG hydrogel encapsulating goat MSCs up to 6 weeks of incubation in osteogenic medium ($P < 0.05$). (E) DNA fraction analysis of PEG hydrogel constructs encapsulating goat MSCs and incubated in osteogenic medium revealed approximately consistent cell survival rates over the 6-week incubation period.

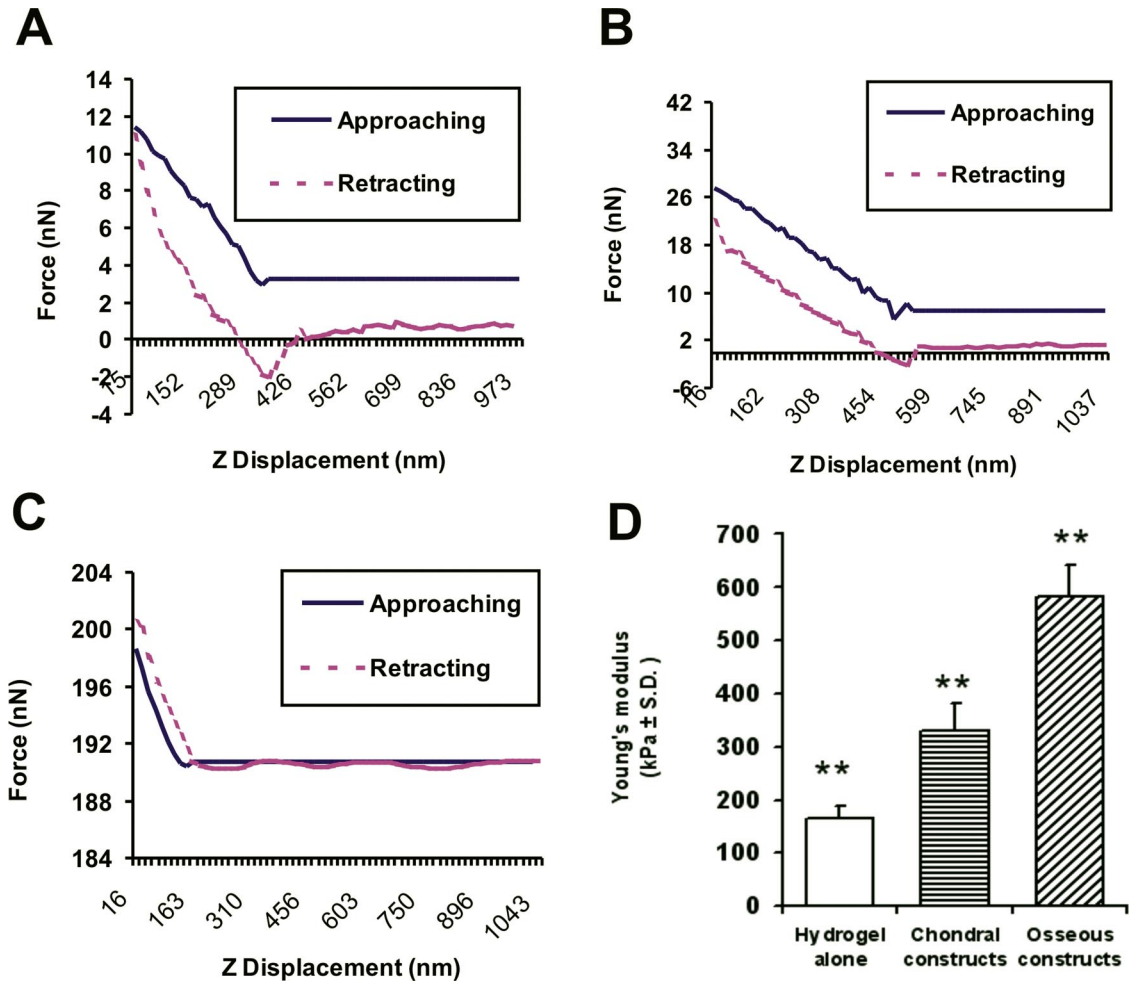

FIGURE 7. Nanomechanical properties of PEG-based hydrogel constructs encapsulating rat MSC-derived chondrogenic and osteogenic cells upon nanoindentation with atomic force microscope (AFM). (A–C) Representative force curves showing nanoscale adhesive forces upon approaching and retracting phases of the AFM scanning tip from the sample surface. Upon nanoindentation of PEG-hydrogel encapsulating rat MSC-derived chondrogenic cells after 4-week incubation (B), the nanoindentation forces required to indent the surface were approximately twofold higher than PEG hydrogel alone (A). Nanoindentation forces for PEG hydrogel encapsulating MSC-derived osteogenic cells after 4-week incubation (C) were higher than PEG hydrogel alone in "A." (D) The mean Young's modulus of the osteogenic PEG hydrogel (*N* = 8) was significantly higher than the chondrogenic PEG hydrogel (*N* = 12) (*P* < 0.01), both of which were significantly higher than PEG hydrogel without cells (*N* = 9) (*P* < 0.01).

and osseous tissues.[5] However, the phenomenon described by Alsberg *et al.*[5] of multiple growth-plate-like organizations within the cartilagenous layer was not replicated in the present work possibly due to different cell sources and their maturation levels prior to *in vivo* implantation. Since the therapeutic targets for tissue-engineered articular condyles are primarily individuals in need of total condylar replacement, we have directed our emphasis toward maintaining chondrogenic and osteogenic phenotypes rather than to imitating the growth potentials. In support of the present approach, chondrogenic and osteogenic phenotypes have also been demonstrated in hyaluronan sponges and ceramic cubes, respectively, by seeding both carriers with rat marrow derived MSCs.[21] Although both chondrogenic and osteogenic components retained a single integrated structure after *in vivo* implantation in syngeneic rats, fibrous tissue band spanned the interface between the two materials with bone formation mostly in the ceramic pores near the periphery.[21] These observations are potentially justification for the present use of PEGDA, or a similar system, to fabricate the tissue-engineered osteochondral constructs. The use of one hydrogel system for both chondrogenic and osteogenic components eliminates the need for biological sealants that may degrade and allow fibrous tissue invasion between chondral and osseous layers. In addition, presumably homogenous cell distribution of encapsulating MSC-derived cells in the aqueous phase of the hydrogel system likely facilitates tissue formation throughout the constructs in comparison with tissue ingrowth from the surface of prefabricated 3D scaffolds.

Several issues must be addressed prior to application of *ex vivo* fabricated tissue-engineered osteochondral constructs directly to a human being in need of total joint replacement. First, chondral and osseous tissue-forming cells must be autologous. In our previous work, we have induced autologous rabbit MSCs, extracted by needle aspiration from bone marrow, to differentiate into chondrogenic and osteogenic cells.[8,61] Second, the degradation rate of PEG-based hydrogel encapsulating MSC-derived chondrogenic and osteogenic cells needs to be optimized to coincide with the rate of *in vivo* histogenesis of cartilage and subchondral bone.[16] Third, growth factor delivery through controlled release technology as in our previous work[17,29,32] may prove to be necessary to maintain phenotypic differentiation of chondrogenic and osteogenic cells. In particular, the presence of few mineral deposits within the chondrogenic layer near the interface (cf., Fig. 3(A)) that might reflect sparse osteogenesis in the chondrogenic layer near the tissue-engineered osteochondral junction, perhaps accentuates the necessity to maintain phenotypic differentiation within each layer. Alternatively, these sparse mineralization spots in the chondrogenic layer near the tissue-engineered osteochondral junction are attributable to interactive diffusion of extracellular components across the interface between the two layers. This latter assumption is reinforced by our observation that such mineral deposits are near the osteochondral interface but not farther into the chondrogenic layer. Interactive diffusion between the chondrogenic and osteogenic layers, if it is indeed the case, is perhaps a positive observation since long-term success of the tissue-engineered articular condyles likely would have synergetic diffusive interactions between the chondrogenic and osteogenic layers. Finally, the most challenging task appears to be mechanical enablement of *ex vivo* fabricated osteochondral constructs to withstand mechanical loading as normal condyles.[3] Mechanical stresses with tailored peak magnitude and frequencies are capable of modulating bone and cartilage growth at different levels of organization.[13,25,27,36,64] Recent evidence indicates that simulated microgravity by bioreactors affects the expression of chondral differentiation markers in cartilage constructs.[51] The present nanomechanical data are instructive in that upon 4-week *ex vivo* incubation, osteogenic constructs demonstrated significantly higher Young's modulus than chondrogenic constructs using atomic force microscopy. The reported nanomechanical values for the osteogenic and chondrogenic constructs are comparable to those of the neonatal articular condyle,[49] but certainly need to be further enhanced for eventual therapeutic applications. Comparison of *ex vivo* biochemical data with histologic phenotypes of *in vivo* samples suggests potentially large increases in mechanical properties after *in vivo* implantation. Both MSC-derived chondrogenic and osteogenic cells, once exposed to appropriate mechanical cues, will likely increase matrix synthesis at accelerated rates and thus may further improve the mechanical properties of tissue-engineered osteochondral constructs.

MSC-derived chondrogenic and osteogenic cells in the present study have apparently survived photopolymerization in a human articular condyle mold with a geometric dimension of $11 \times 6 \times 7$ mm ($l \times w \times h$). The encapsulation density of MSC-derived chondrogenic and osteogenic cells was both 5×10^6/ml. Although the present *in vivo* chondrogenesis and osteogenesis have been driven separately by MSCs induced to differentiate into chondrogenic and osteogenic lineages *in vitro*, a question arises as to what are the optimal densities of MSC-derived chondrogenic and osteogenic cells for maximizing the regenerative outcome of tissue-engineered articular condyles. Sparse chondrocyte-like cells in the chondrogenic layer of the harvested articular condyle likely indicate a necessity to increase cell encapsulation densities, although chondrocytes only account for approximately 5% volume in the adult native cartilage.[59] In spite of paucity of cell density studies using PEG hydrogel for osteochondral constructs, previous work using other hydrogel systems is instructive. For instance, the regenerative outcome of the articular disc of the mandibular joint appears to be a function of increasing cell density up to 100×10^6 cells/ml.[54] More mineral deposits are observed with 8×10^3 cells/cm^2 than 2.6×10^3 cells/cm^2 of marrow-derived cells.[24] Thus, greater encapsulation densities for MSC-derived chondrogenic and osteogenic cells in the present PEG-based hydrogel appear to be warranted. The potentially suboptimal cell-seeding density, along with relatively short *ex vivo* incubation periods, likely is also responsible for the suboptimal GAG and collagen contents of the present chondrogenic constructs, although one should also consider the degradation rate of the presently used PEG-based hydrogel and its effects on the rate of matrix synthesis by MSC-derived chondrogenic cells. Nonetheless, the currently measured biochemical values are comparable with those observed in tissue-engineered cartilage[16,54,57] and bone[11,57] constructs using isolated chondrocytes and osteoblasts.

The presently used uniform scaffold, poly(ethylene glycol)-diacrylate, is capable of maintaining phenotypic differentiation of MSC-derived chondrogenic and osteogenic cells in two stratified and yet integrated layers both *ex vivo* and *in vivo*. PEGDA is biocompatible and FDA approved for several medical applications.[20] Photopolymerization offers several advantages over other polymerization techniques.[41,48] A uniform scaffold has the advantage over copolymers for the ease of material integration, *ex vivo* fabrication, and sterilization.[16,41] The division between chondrogenic and osteogenic layers may prove to be advantageous in allowing separate phenotypic differentiations, although chondrocyte degeneration and osteoblast invasion are required as in natural osteochondral junction.

As in a previous attempt to fabricate composite tissue constructs,[5] the present multifaceted data from stem cell biology, RNA and DNA assays, biochemical, histological,

and nanomechanical approaches were obtained from two species: rat MSCs and goat MSCs, both encapsulated using the same PEG-based hydrogel protocols. This reflects the necessary collaboration often needed for an orchestrated tissue-engineering effort, which may extend from cell and molecular biology, biomaterials, biomechanics to animal models.[46,63] Performance of mRNA and biochemical assays on *ex vivo* incubated samples, instead of *in vivo* samples, was necessitated by the fact that *in vivo* osteochondral constructs would compromise these assays due to their demonstrated cartilaginous and osseous tissue phenotypes. Additional assays such as immunohistochemistry and/or laser dissection microscopy would be useful to overcome this difficulty. Moreover, once osteochondral constructs are fabricated *ex vivo*, it is necessary to maintain the differentiation state of both MSC-derived chondrogenic and osteogenic cells by incubating them with corresponding chondrogenic and osteogenic culture medium, respectively. This objective is, however, technically infeasible due to the unpredictability that might result from combining two different specially formulated media in a single culture. The observed differentiations of MSCs into chondrogenic and osteogenic cells are based on the premise that MSCs from multiple species are capable of differentiating into all connective tissue cells.[44,47,52] The ultimate goal of *ex vivo* fabrication of human articular condyles from autologous human MSCs is likely facilitated, rather than hindered, by parallel optimization approaches utilizing multispecies MSCs. Taken together, the present *in vitro* and *in vivo* data indicate maintenance of chondrogenic and osteogenic lineages of adult mesenchymal stem cells exposed to chondrogenic and osteogenic stimulations, and that the induced chondrogenic and osteogenic phenotypes are retained in a human-shaped articular condyle. The present findings may serve as a primitive proof of concept for ultimate tissue-engineered replacement of degenerated articular condyles via a single population of adult mesenchymal stem cells.

ACKNOWLEDGMENTS

We thank Professor Maurizio Pacifici for providing valuable comments on an earlier version of the paper. The present work was supported by Arthritis Investigator Grant from the Arthritis Foundation to J.H.E; NIH grants AR048316, DE00722, and AG00010 to A.I.C; and the IRIB Grant on Biotechnology jointly from the UIC (University of Illinois at Chicago) and UIUC (University of Illinois at Urbana—Champaign), a Biomedical Engineering Research Grant from the Whitaker Foundation (RG-01-0075), and NIH grants DE13964 and EB02332 to J.J.M.

REFERENCES

[1] Abukawa, H., H. Terai, D. Hannouche, J. P. Vacanti, L. B. Kaban, and M. J. Troulis. Formation of a mandibular condyle *in vitro* by tissue engineering. *J. Oral Maxillofac. Surg.* 61:94–100, 2003.

[2] Ahmad, C. S., Z. A. Cohen, W. N. Levine, G. A. Ateshian, and V. C. Mow. Biomechanical and topographic considerations for autologous osteochondral grafting in the knee. *Am. J. Sports Med.* 29:201–206, 2001.

[3] Ahmad, C. S., W. B. Guiney, and C. J. Drinkwater. Evaluation of donor site intrinsic healing response in autologous osteochondral grafting of the knee. *Arthroscopy* 18:95–98, 2002.

[4] Alhadlaq, A., and J. J. Mao. Tissue-engineered neogenesis of human-shaped mandibular condyle from rat mesenchymal stem cells. *J. Dent. Res.* 82:951–956, 2003.

[5] Alsberg, E., K. W. Anderson, A. Albeiruti, J. A. Rowley, and D. J. Mooney. Engineering growing tissues. *Proc. Natl. Acad. Sci. U.S.A.* 17:12025–12030, 2002.

[6] Athanasiou, K. A., A. Agarwal, A. Muffoletto, F. J. Dzida, G. Constantinides, and M. Clem. Biomechanical properties of hip cartilage in experimental animal models. *Clin. Orthop.* 316:254–266, 1995.

[7] Aubin, J. E. Advances in the osteoblast lineage. *Biochem. Cell. Biol.* 76:899–910, 1998.

[8] Awad, H. A., D. L. Butler, G. P. Boivin, F. N. Smith, P. Malaviya, B. Huibregtse, and A. I. Caplan. Autologous mesenchymal stem cell-mediated repair of tendon. *Tissue Eng.* 5:267–277, 1999.

[9] Bentley, G., and R. B. Greer. Homotransplantation of isolated epiphyseal and articular cartilage chondrocytes into joint surfaces of rabbits. *Nature* 230:385–388, 1971.

[10] Bruder, S. P., N. Jaiswal, N. S. Ricalton, J. D. Mosca, K. H. Kraus, and S. Kadiyala. Mesenchymal stem cells in osteobiology and applied bone regeneration. *Clin. Orthop.* 355:247S–256S, 1998.

[11] Burdick, J. A., and K. S. Anseth. Photoencapsulation of osteoblasts in injectable RGD-modified PEG hydrogels for bone tissue engineering. *Biomaterials* 23:4315–4323, 2002.

[12] Caplan, A. I. Mesenchymal stem cells. *J. Orthop. Res.* 9:641, 1991.

[13] Carter, D. R., G. S. Beaupre, N. J. Giori, and J. A. Helms. Mechanobiology of skeletal regeneration. *Clin. Orthop.* 355:41S–55S, 1998.

[14] Caterson, E. J., L. J. Nesti, W. J. Li, K. G. Danielson, T. J. Albert, A. R. Vaccaro, and R. S. Tuan. Three-dimensional cartilage formation by bone marrow-derived cells seeded in polylactide/alginate amalgam. *J. Biomed. Mater. Res.* 57:394–403, 2001.

[15] Deschamps, A. A., D. W. Grijpma, and J. Feijen. Phase separation and physical properties of PEO-containing poly(ether ester amide)s. *J. Biomater. Sci. Polym. Ed.* 13:1337–1352, 2002.

[16] Elisseeff, J., W. McIntosh, K. Anseth, S. Riley, P. Ragan, and R. Langer. Photoencapsulation of chondrocytes in poly(ethylene oxide)-based semi-interpenetrating networks. *J. Biomed. Mater. Res.* 51:164–171, 2000.

[17] Elisseeff, J., W. McIntosh, K. Fu, B. T. Blunk, and R. Langer. Controlled-release of IGF-I and TGF-beta1 in a photopolymerizing hydrogel for cartilage tissue engineering. *J. Orthop. Res.* 19:1098–1104, 2001.

[18] Freed, L. E., D. A. Grande, Z. Lingbin, J. Emmanual, J. C. Marquis, and R. Langer. Joint resurfacing using allograft chondrocytes and synthetic biodegradable polymer scaffolds. *J. Biomed. Mater. Res.* 28:891–899, 1994.

[19] Froimson, M. I., A. Ratcliffe, T. R. Gardner, and V. C. Mow. Differences in patellofemoral joint cartilage material properties and their significance to the etiology of cartilage surface fibrillation. *Osteoarth. Cartil.* 5:377–386, 1997.

[20] Fu, J., J. Fiegel, E. Krauland, and J. Hanes. New polymeric carriers for controlled drug delivery following inhalation or injection. *Biomaterials* 23:4425–4433, 2002.

[21]Gao, J., J. E. Dennis, L. A. Solchaga, A. S. Awadallah, V. M. Goldberg, and A. I. Caplan. Tissue-engineered fabrication of an osteochondral composite graft using rat bone marrow-derived mesenchymal stem cells. *Tissue Eng.* 7:363–371, 2001.
[22]Gay, S., S. Kuchen, R. E. Gay, and M. Neidhart. Cartilage destruction in rheumatoid arthritis. *Ann. Rheum. Dis.* 61:87, 2002.
[23]Goldberg, V. M., and A. I. Caplan. Biological resurfacing: An alternative to total joint arthroplasty. *Orthopedics* 17:819–821, 1994.
[24]Goldstein, A. S. Effects of cell concentration and growth period on articular and ear chondrocyte transplants for tissue engineering. *Plast. Reconstr. Surg.* 108:392–402, 2001.
[25]Goldstein, S. A. Tissue engineering: Functional assessment and clinical outcome. *Ann. N.Y. Acad. Sci.* 961:183–192, 2002.
[26]Gravallese, E. M. Bone destruction in arthritis. *Ann. Rheum. Dis.* 61:84–86, 2002.
[27]Grodzinsky, A. J., M. E. Levenston, M. Jin, and E. H. Frank. Cartilage tissue remodeling in response to mechanical forces. *Ann. Rev. Biomed. Eng.* 2:691–713, 2000.
[28]Guilak, F., and V. C. Mow. The mechanical environment of the chondrocyte: A biphasic finite element model of cell–matrix interactions in articular cartilage. *J. Biomech.* 33:1663–1673, 2000.
[29]Hanada, K., L. A. Solchaga, A. I. Caplan, T. M. Hering, V. M. Goldberg, J. U. Yoo, and B. Johnstone. BMP-2 induction and TGF-beta1 modulation of rat periosteal cell chondrogenesis. *J. Cell. Biochem.* 81:284–294, 2001.
[30]Hangody, L., P. Feczko, L. Bartha, G. Bodo, and G. Kish. Mosaicplasty for the treatment of articular defects of the knee and ankle. *Clin. Orthop.* 391:328S–336S, 2001.
[31]Hollinger, J. O., J. M. Schmitt, D. C. Buck, R. Shannon, S. P. Joh, H. D. Zegzula, and J. Wozney. Recombinant human bone morphogenetic protein-2 and collagen for bone regeneration. *J. Biomed. Mater. Res.* 43:356–364, 1998.
[32]Hong, L., S. Miyamoto, N. Hashimoto, and Y. Tabata. Synergistic effect of gelatin microspheres incorporating TGF-beta1 and a physical barrier for fibrous tissue infiltration on skull bone formation. *J. Biomater. Sci. Polym. Ed.* 11:1357–1369, 2000.
[33]Hu, K., P. Radhakrishnan, R. V. Patel, and J. J. Mao. Regional structural and viscoelastic properties of fibrocartilage upon dynamic nanoindentation of the articular condyle. *J. Struct. Biol.* 136:470–475, 2001.
[34]Hunziker, E. B. Articular cartilage repair: Basic science and clinical progress. A review of the current status and prospects. *Osteoarth. Cartil.* 10:432–463, 2002.
[35]Isogai, N., W. Landis, T. H. Kim, L. C. Gerstenfeld, J. Upton, and J. P. Vacanti. Formation of phalanges and small joints by tissue-engineering. *J. Bone Joint Surg. Am.* 81:306–316, 1999.
[36]Kopher, R. A., and J. J. Mao. Sutural growth modulated by the oscillatory component of micromechanical strain. *J. Bone Miner. Res.* 18:521–528, 2003.
[37]Korhonen, R. K., M. S. Laasanen, J. Toyras, J. Rieppo, J. Hirvonen, H. J. Helminen, and J. S. Jurvelin. Comparison of the equilibrium response of articular cartilage in unconfined compression, confined compression and indentation. *J. Biomech.* 35:903–909, 2002.
[38]Krebsbach, P. H., S. A. Kuznetsov, P. Bianco, and P. G. Robey. Bone marrow stromal cells: Characterization and clinical application. *Crit. Rev. Oral Biol. Med.* 10:165–181, 1999.
[39]Lammi, M., and M. Tammi. Densitometric assay of nanogram quantities of proteoglycans precipitated on nitrocellulose membrane with safranin O. *Anal. Biochem.* 168:352–357, 1988.
[40]Langer, R. S., and J. P. Vacanti. Tissue engineering: The challenges ahead. *Science* 280:86–89, 1999.
[41]Lee, K. Y., and D. J. Mooney. Hydrogels for tissue engineering. *Chem. Rev.* 101:1869–1879, 2001.
[42]Lietman, S. A., S. Miyamoto, P. R. Brown, N. Inoue, and A. H. Reddi. The temporal sequence of spontaneous repair of osteochondral defects in the knees of rabbits is dependent on the geometry of the defect. *J. Bone Joint Surg. Br.* 84:600–606, 2002.
[43]Lutolf, M. P., F. E. Weber, H. G. Schmoekel, J. C. Schense, T. Kohler, R. Muller, and J. A. Hubbell. Repair of bone defects using synthetic mimetics of collagenous extracellular matrices. *Nat. Biotechnol.* 21:513–518, 2003.
[44]MacKenzie, T. C., and A. W. Flake. Human mesenchymal stem cells: Insights from a surrogate *in vivo* assay system. *Cells Tissues Organs* 171:90–95, 2002.
[45]Martin, R. B., D. B. Burr, and N. A. Sharkey. Skeletal Tissue Mechanics. New York: Springer-Verlag, 1998.
[46]Mooney, D. J., and A. G. Mikos. Growing new organs. *Science* 280:60–65, 1999.
[47]Naumann, A., J. E. Dennis, A. Awadallah, D. A. Carrino, J. M. Mansour, E. Kastenbauer, and A. I. Caplan. Immunochemical and mechanical characterization of cartilage subtypes in rabbit. *J. Histochem. Cytochem.* 50:1049–1058, 2002.
[48]Nguyen, K. T., and J. L. West. Photopolymerizable hydrogels for tissue engineering applications. *Biomaterials* 23:4307–4314, 2002.
[49]Patel, R. V., and J. J. Mao. Microstructural and elastic properties of the extracellular matrices of the superficial zone of neonatal articular cartilage by atomic force microscopy. *Front. Biosci.* 8:18–25, 2003.
[50]Peacock, M., C. H. Turner, M. J. Econs, and T. Foroud. Genetics of osteoporosis. *Endocr. Rev.* 23:303–326, 2002.
[51]Pei, M., L. A. Solchaga, J. Seidel, L. Zeng, G. Vunjak-Novakovic, A. I. Caplan, and L. E. Freed. Bioreactors mediate the effectiveness of tissue engineering scaffolds. *FASEB J.* 16:1691–1694, 2002.
[52]Pelled, G., H. Aslan, Z. Gazit, and D. Gazit. Mesenchymal stem cells for bone gene therapy and tissue engineering. *Curr. Pharm. Des.* 8:1917–1928, 2002.
[53]Pittenger, M. F., A. M. Mackay, S. C. Beck, R. K. Jaiswal, R. Douglas, J. D. Mosca, M. A. Moorman, D. W. Simonetti, S. Craig, and D. R. Marshak. Multilineage potential of adult human mesenchymal stem cells. *Science* 284:143–147, 1999.
[54]Puelacher, W. C., J. Wisser, C. A. Vacanti, N. F. Ferraro, D. Jaramillo, and J. P. Vacanti. Temporomandibular joint disc replacement made by tissue-engineered growth of cartilage. *J. Oral Maxillofac. Surg.* 52:1172–1177, 1994.
[55]Roder, C., S. Eggli, M. Aebi, and A. Busato. The validity of clinical examination in the diagnosis of loosening of components in total hip arthroplasty. *J. Bone Joint Surg. Br.* 85:37–44, 2003.
[56]Schaefer, D., I. Martin, G. Jundt, J. Seidel, M. Heberer, A. Grodzinsky, I. Bergin, G. Vunjak-Novakovic, and L. E. Freed. Tissue-engineered composites for the repair of large osteochondral defects. *Arthritis Rheum.* 46:2524–2534, 2002.
[57]Schaefer, D., I. Martin, P. Shastri, R. F. Padera, R. Langer, L. E. Freed, and G. Vunjak-Novakovic. *In vitro* generation of osteochondral composites. *Biomaterials* 21:2599–2606, 2000.
[58]Sikavitsas, V. I., G. N. Bancroft, and A. G. Mikos. Formation of three-dimensional cell/polymer constructs for bone tissue engineering in a spinner flask and a rotating wall vessel bioreactor. *J. Biomed. Mater. Res.* 62:136–148, 2002.
[59]Shum, L., and G. Nuckolls. The life cycle of chondrocytes in the developing skeleton. *Arthritis Res.* 4:94–106, 2002.
[60]Solchaga, L. A., J. Gao, J. E. Dennis, A. Awadallah, M. Lundberg, A. I. Caplan, and V. M. Goldberg. Treatment of

osteochondral defects with autologous bone marrow in a hyaluronan-based delivery vehicle. *Tissue Eng.* 8:333–347, 2002.

[61]Tabata, Y., L. Hong, S. Miyamoto, M. Miyao, N. Hashimoto, and Y. Ikada. Bone formation at a rabbit skull defect by autologous bone marrow cells combined with gelatin microspheres containing TGF-beta1. *J. Biomater. Sci. Polym. Ed.* 11:891–901, 2000.

[62]Vacanti, C. A., W. Kim, B. Schloo, J. Upton, and J. P. Vacanti. Joint resurfacing with cartilage grown in situ from cell-polymer structures. *Am. J. Sports Med.* 22:485–488, 1994.

[63]Vacanti, J. P., and R. Langer. Tissue engineering: The design and fabrication of living replacement devices for surgical reconstruction and transplantation. *Lancet* 354:132S–134S, 1999.

[64]Wang, X., and J. J. Mao. Accelerated chondrogenesis of the rabbit cranial base growth plate upon oscillatory mechanical stimuli. *J. Bone Miner. Res.* 17:457–462, 2002.

[65]Winn, S. R., J. M. Schmitt, D. Buck, Y. Hu, D. Grainger, and J. O. Hollinger. Tissue-engineered bone biomimetic to regenerate calvarial critical-sized defects in athymic rats. *J. Biomed. Mater. Res.* 45:414–421, 1999.

[66]Zysset, P. K., X. E. Guo, C. E. Hoffler, K. E. Moore, and S. A. Goldstein. Elastic modulus and hardness of cortical and trabecular bone lamellae measured by nanoindentation in the human femur. *J. Biomech.* 32:1005–1012, 1999.